412 *Chemistry of Materials* 1989, *1*, 412–420

# Structural Trends in Potential Organic Conductors Based on (Donor–$CH_2$)$_2$ Tetracyanoquinodimethane Molecules

J. Y. Becker, J. Bernstein,* S. Bittner, J. A. R. P. Sarma,* and S. S. Shaik

*The Organic Metals Group, Department of Chemistry, Ben-Gurion University of the Negev, Beer Sheva 84120, Israel*

*Received February 8, 1989*

The stoichiometry of electron donor–acceptor (EDA) complexes with potential electrical conductivity may be predetermined by preparing compounds in which D(s) and A(s) are chemically linked. The structural properties of three compounds comprised of two identical Ds bonded to one A (TCNQ; i.e., D···A···D) are reported here. The three compounds are isostructural; monoclinic, space group $P2_1/a$, $Z = 2$. D = $C_6H_5$: $a = 13.999$ (6), $b = 10.760$ (2), $c = 6.970$ (2) Å, $\beta = 102.51$ (3)°. D = $p$-$C_6H_4OCH_3$: $a = 16.887$ (6), $b = 10.235$ (6), $c = 7.172$ (4) Å, $\beta = 107.80$ (4)°. D = $\beta$-naphthyl: $a = 16.93$ (4), $b = 11.676$ (8), $c = 7.093$ (9) Å, $\beta = 114.3$ (1)°. The structure of the last compound has also been determined at 93 K: $a = 16.816$ (5), $b = 11.438$ (4), $c = 7.086$ (1) Å, $\beta = 115.21$ (3)°. The outstanding common structural feature is the tendency to form infinite segregated stacks of A along the $c$ axis, thus achieving a condition necessary for electrical conductivity. The charge-transfer interaction is achieved by the formation of previously not observed D···A···D triplets along both the A stacks and linking screw-related stacks. Details of the interactions leading to this unusual architecture are investigated with the aid of lattice energy calculations.

## Introduction

The preparation of electrically conducting organic materials made of $\pi$-electron donor–acceptor (EDA) complexes depends on a small number of electronic and structural requirements,[1,2] which must be met simultaneously. We have reasoned[1] that molecules of the general formula $D_m$–$A_n$ (1), where D and A are $\pi$-electron donor and acceptor, respectively, and $m$ and $n$ are integers, are endowed with sufficient flexibility to attempt eventually to optimize all the key factors simultaneously. However, prior to such an attempt we felt that a methodical study of each factor was a necessary condition to establish a reliable structure–conductivity relationship.[3]

One of the key requirements is the presence of segregated $D_\infty$ and $A_\infty$ stacks in the three dimensional architecture.[2] These stacks are required because overlap of the $\pi$-orbitals leads to development of the energy bands for the conduction electrons (which should *eventually* be generated through a *redox* process). We have decided therefore to focus attention on this architectural requirement and to study and develop ways in which segregated stacking can be predesigned.

Along these lines, we have recently prepared[3] a "family" of compounds of the formula $D_2A$, which belongs to the general type 1. This family is shown in 2 and involves a TCNQ unit as the acceptor and various aryl groups as donors. Our primitive reasoning was that this prototype should exhibit segregated stacking for close packing reasons, which indeed it does in quite a unique way as schematically shown in 3.[1] Here, we show the $c$ direction in the crystal structure of the derivative with D = $C_6H_5$.[1]

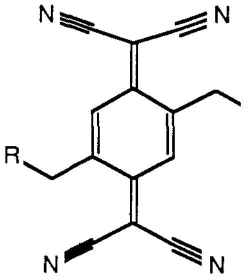

2a: R = $C_6H_5$-
2b: R = $p$-$OCH_3$-$C_6H_4$-
2c: R = β-Naphthyl-

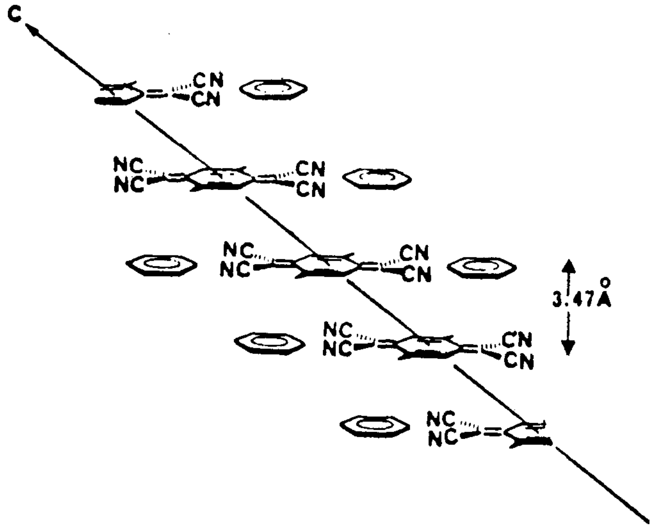

3

Thus, the (D–$CH_2$–)$_2$TCNQ molecule possesses an infinite stack of TCNQ moieties flanked, from top and bottom, by D units from neighboring stacks. This feature has been found to be common to the entire family of 2, whose solids are crystallographically isostructural, independent of the nature of D. The isomorphism suggests that the stacking is not an anomaly but rather a characteristic packing arrangement which merits understanding, in line with our general plan.

Now this isostructurality provides a unique opportunity to study the various interactions resulting from chemical modification under conditions of a fixed architecture. This is what we attempt to do in this paper. Thus, we report here the detailed crystal structures and the results of packing energy analyses.

## Experimental Section

**Crystal Structure Determination.** The syntheses of **2a–c** have been described earlier.[3] Crystals of quality suitable for single-crystal X-ray diffraction experiments were obtained by slow evaporation from chlorobenzene. The crystals of compound **2a** are orange and transparent, while those of **2b** and **2c** are dark

---

(1) Becker, J. Y.; Bernstein, J.; Bittner, B.; Levi, N.; Shaik, S. S. *J. Am. Chem. Soc.* **1983**, *105*, 4468.

(2) Shaik, S. S. *J. Am. Chem. Soc.* **1982**, *104*, 5328.

(3) Becker, J. Y.; Bernstein, J.; Bittner, B.; Levi, N.; Shaik, S. S.; Zer-Zion, N. *J. Org. Chem.* **1988**, *53*, 1694.

0897-4756/89/2801-0412$01.50/0

**Table I. Crystallographic Data for Compounds 2a–c.**

|  | **2a** | **2b** | **2c** | **2c** (at 93 K) |
|---|---|---|---|---|
| mol formula | $C_{26}H_{16}N_4$ | $C_{28}H_{20}N_4O_2$ | $C_{34}H_{20}N_4$ | $C_{34}H_{20}N_4$ |
| MW | 384 | 444 | 474 | 474 |
| cryst size, in mm | 0.25 × 0.28 × 0.32 | 0.21 × 0.30 × 0.60 | 0.09 × 0.21 × 0.24 | 0.09 × 0.21 × 0.24 |
| cryst syst | monoclinic | monoclinic | monoclinic | monoclinic |
| space group | $P2_1/a$ | $P2_1/a$ | $P2_1/a$ | $P2_1/a$ |
| $a$, Å | 13.999 (6) | 16.877 (6) | 16.93 (4) | 16.816 (5) |
| $b$, Å | 10.760 (2) | 10.235 (6) | 11.676 (8) | 11.438 (4) |
| $c$, Å | 6.970 (2) | 7.172 (4) | 7.093 (9) | 7.086 (1) |
| $\beta$, deg | 102.51 (3) | 107.80 (4) | 114.3 (1) | 115.21 (3) |
| $V$, Å$^3$ | 1024.9 (5) | 1179.6 (10) | 1278 (3) | 1233.1 (3) |
| $Z$ | 2 | 2 | 2 | 2 |
| $F(000)$ | 400 | 464 | 504 | 504 |
| $\mu$ (Mo K$\alpha$), cm$^{-1}$ | 0.41 | 0.46 | 0.41 | 5.31$^b$ |
| $D_c$, g cm$^{-3}$ | 1.25 | 1.25 | 1.23 | 1.28 |
| $D_m$, g cm$^{-3}$ | 1.23 | 1.24 | 1.24 |  |
| no. of unique reflctns | 1564 | 1704 | 1492 | 1946 |
| no. of reflcns used in refinements | $1235 \geq 3\sigma$ | $888 \geq 4\sigma$ | $764 \geq 4\sigma$ | $1547 \geq 3\sigma$ |
| $R$ | 0.071 | 0.086 | 0.085 | 0.072 |
| $R_w$ | 0.071 | 0.088 | 0.086 | 0.072 |
| weighting factor | unit weights | $a$ | $a$ | $a$ |
| reflctns omitted | 2 2 1;<br>1 2 1;<br>2 9 1;<br>1 13 1;<br>1 2 −3 | 2 0 0;<br>1 2 0;<br>0 1 1;<br>2 1 1;<br>2 1 −1 | 0 0 1;<br>2 2 1;<br>1 2 1;<br>0 3 1;<br>0 3 5 | 1 1 0;<br>2 1 0;<br>−2 0 2;<br>0 0 2;<br>0 1 3 |

[a] General weighting factor = $\{c/[\sigma^2(F_o) + (kF_o)^2]\}$: **2b**, $c = 2.3273$, $k = 0.02$; **2c**, $c = 1.4607$, $k = 0.059$; **2c** (at 93 K) $c = 1.0248$, $k = 0.02$. [b] $\mu$(Cu K$\alpha$).

violet and opaque. The three compounds are isomorphous, exhibiting {110}, {101}, and {001} forms and occasionally some less developed faces of the {111} type. The crystallographic data for all compounds are given in Table I. Unit-cell parameters for the three compounds were determined by a least-squares fit of 15 accurately centered high-order reflections within limits $12 < 2\theta < 30°$. The low-temperature data set was collected on a Rigaku four-circle diffractometer using Cu K$\alpha$ radiation; the room-temperature data sets were collected on a Syntex $P\bar{1}$ four-circle automated diffractometer using Mo K$\alpha$ radiation, graphite monochromator with the $\theta/2\theta$ scan technique to a maximum $2\theta$ of 50°. Three reflections were monitored at intervals of 60 measurements. For the room-temperature data of compound **2c**, the data were collected on two equivalent quadrants and merged. No absorption corrections were applied, and there was no evidence for crystal decomposition during the data collection. Lorentz and polarization corrections were applied. Averaging of equivalent reflections gave the total number of unique reflections listed in Table I. The similarity in parameters and space groups indicate that the three compounds are isostructural.

The three structures were solved by direct methods, and the initial least-squares refinement for six cycles with unit weights on compounds **2a**–**2c** and **2c** (low temperature) commenced at $R$ values of 0.28, 0.32, 0.40, and 0.42 and converged to 0.14, 0.17, 0.16, and 0.12, respectively. In the case of the room-temperature data sets, refinement was continued with all non-hydrogen atoms anisotropic and the $R$ values dropped to 0.10, 0.13, and 0.13, respectively. At this stage, the difference Fourier maps revealed the positions of all hydrogen atoms except H12 in compound **2b**, which was fixed and "tied" to C12 throughout further refinements. All hydrogen atoms that were considered as isotropic and anisotropic non-hydrogen atoms were refined by block-diagonal least-squares with half of a TCNQ in one block and the donor unit in a second block, and the $R$ factors converged to 0.076, 0.088, and 0.995, respectively. In the case of the low-temperature data set, after the initial six cycles of isotropic refinements all the hydrogens were located in the difference map and were included in the next refinement with all non-hydrogen atoms for six more cycles, and the $R$ factor converged to a value of 0.10. In the next stage all the non-hydrogen atoms were refined anisotropically along with isotropic hydrogen atoms in a fixed block which produced an $R$ factor of 0.077. At this stage a weighting scheme was applied in all the four cases and in each case about five reflections which exhibited signs of extinction were removed. The final $R$ and $R_w$ factors and weighting schemes are given in Table I. Final positional parameters and equivalent isotropic thermal parameters are listed in Table II.

The structures were solved with SHELX86[4] and SHELX76,[4] and the latter was used for refinement. Geometry calculations were done by GEOM[5] and GEOM78.[6] Illustrations were prepared with PLUTO78[6] and ORTEP.[7] Temperature factors, torsion angles, and structure factors for all three compounds have been deposited as supplementary material (see the paragraph at the end of the paper).

**Lattice Energy Minimizations.** The lattice energy minimizations were carried out with SYMM[8] and PCK83.[9] Dependence of the results on potential function and parameters was tested by carrying out some of the calculations with 6–12 (Lennard-Jones)[22] and Mirsky[23] potentials, including electrostatic contributions.

Although the absolute values of computed energy changed when either of the latter two potentials were used, the same trends were observed in all calculations. For the electrostatic contribution charges were assigned to the atoms on the basis of a Mulliken analysis of extended Hückel calculations (carried out with ICON8[10] including the charge-iteration option). Similar values for the charges were obtained from bond moments at the minimum energy molecular conformation based on a molecular mechanics calculations.[24] Typical values are ca. $-0.48e^-$ on the nitrile nitrogen, $0.26e^-$ on the nitrile carbon and $-0.61e^-$ on the methoxy oxygen of **2b**, which also includes the electrostatic contributions to the total energy, final cell parametes with the shifts from the observed values, and the energy contributions to the total from various neighboring molecules and individual atoms.

## Results and Discussion

**Molecular Structures of the TCNQ and Donor Moieties.** In spite of substituents that differ in size and donor capability on the TCNQ moiety, the three compounds are isostructural. The molecules are centrosymmetric, i.e., the center of symmetry coincides with the origin of the unit cell. Figure 1 shows the atomic numbering scheme and other features of the molecular geometry, and the ORTEP diagrams are given in Figure 2. Bond lengths and bond angles are given in Tables III and IV, respectively, and the derived information on best planes is given in Table V.

The dimensions of the dicyanomethane group are very similar in **2a** and **2c**;[11] those for **2b** differ at just about the level of statistical significance. The tabulated values may be compared with TCNQ for which the averaged corresponding values for crystallographically independent cyano groups are 1.140 (3) Å and 179.5 (2)° (Table III).[12] For **2a**–**c** the bond angles around C3 (Table III) are almost the same, with C1–C3–C4 being smaller while C2–C3–C4 is larger than in neat TCNQ. If viewed simply as 2,5-di-

---

[4] Sheldrick, G. M. SHELX86, a Crystallographic Structure Solution Package; SHELX76, a Crystallographic Structure Solution and Refinement Package; University of Gottingen: Gottingen, 1986.

[5] Gilmore, C. GEOM, a Program for Calculation of Molecular and Crystal Geometry; Glasgow University: Glasgow, Scotland.

[6] Motherwell, S. GEOM78, PLUTO78; Cambridge University: Cambridge, England, 1978.

[7] Johnson, C. K. ORTEP; Report No. ORNL-3794; Oak Ridge National Laboratory: Oak Ridge, TN, 1965.

[8] Hagler, A. T. SYMM, a Program for Lattic Energy Minimizations; Weizmann Institute of Science: Rehovoth, Israel, 1975.

[9] Williams, D. E. PCK83, a Program for Calculation of Crystal Packing and Nonbonded Forces; University of Louisville: Louisville, KY, 1983.

[10] ICON, a Program for performing Extended Hückel calculations including charge iteration; Quantum Chemistry Program Exchange, Department of Chemistry, Indiana University, Bloomington, IN 47405.

[11] In the text that follows the values in brackets are those obtained from the low-temperature data of **2c**.

[12] Long, R. E.; Sparks, R. A.; Trueblood, K. N. *Acta Crystallogr.* **1965**, *18*, 932.

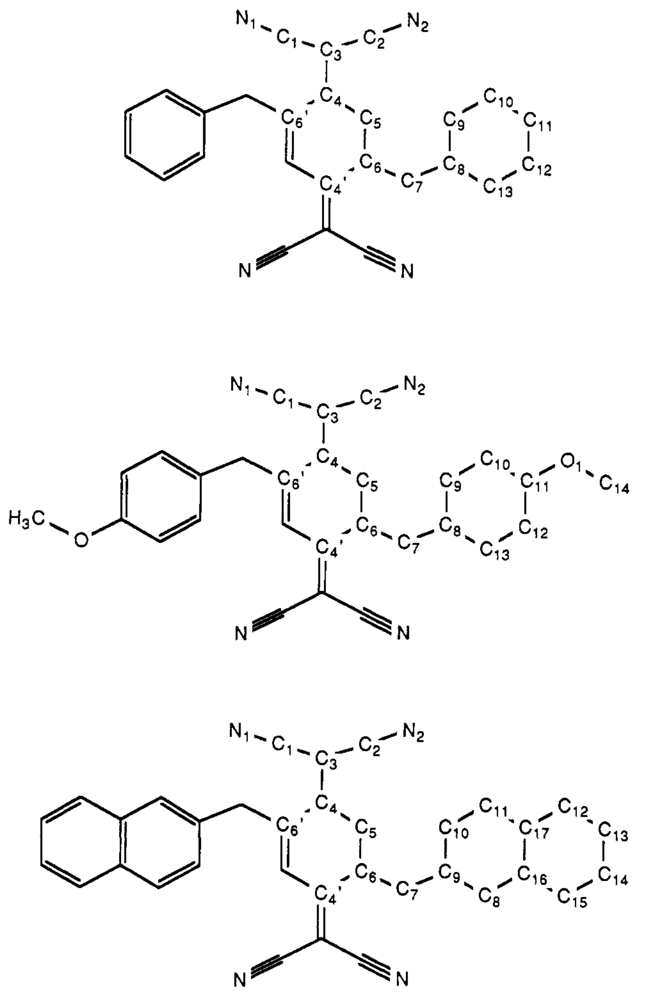

**Figure 1.** Molecules **2a**, **2b**, and **2c** showing the atomic numbering scheme. Hydrogens are numbered according to the carbon atoms to which they are bonded.

substituted TCNQs, these molecules **2a–c** contain some of the bulkiest substituents yet attached to TCNQ. The substituents do not lead to any significant changes in bond lengths, but there are apparently some consistent trends in the perturbation of bond angles in the dicyanomethane group from nominal values. In all cases the geometric parameters of the cyano group in closer proximity to the substituent on TCNQ are more perturbed from the geometry found in unsubstituted TCNQ.

As expected from the isostructural situation, there is generally a constancy of molecular geometry, the most prominent feature being the near-perpendicular arrangement of donors with respect to the plane of the acceptor (Figure 3 and Table V). The presence of intramolecular strain is manifested in the angles between the quinonoid ring (plane 3, Table V) on one hand and the dicyanomethylene group (plane 1) and the methylene group to the donor (plane 2) on the other hand. **2b** is distinguished from the other two compounds by the out-of-plane rotation of the methoxy group by 25°, and the largest values for the rotations noted above occur for this compound. The methylene bridge is significantly out of the plane of the acceptor; this could lead to somewhat reduced steric interaction in this region of the molecule, and relevant geometric parameters, while only just above the level of significance, are consistent with such an interpretation. We believe that there are specific packing effects operating here, and these will be discussed below.

**Description of the Three-Dimensional Crystal Structures of 2a–c.** Let us turn now to the structural details of **2a–c** which are schematized in **3**. The remarkable feature of these three structures is that the central A (A = TCNQ) units of the D- -A- -D molecule form slipped segregated stacks along the *c*-axis direction leading to a uniform interplanar A···A distance of 3.48 (9) Å. The crystal structures are represented in Figure 3 by the packing diagram of **2a**. The packing is in stark constrast to the structure of TCNQ itself (Figure 4) in which there is no overlap between the short-axis *b*-translated molecules even though the axial length is virtually identical with the *c* axis in **2a**. This A···A overlap in **2a–c** is due to overlapping $(CN)_2C\cdots C(CN)_2$ groups (Figure 3) rather than the usual ring···ring or ring···double bond types often found in the segregated stack TCNQ complexes.[13] As shown in **4** taking **2a** as an example, in the region of overlapping dicyano methide groups, in all three compounds, there exist

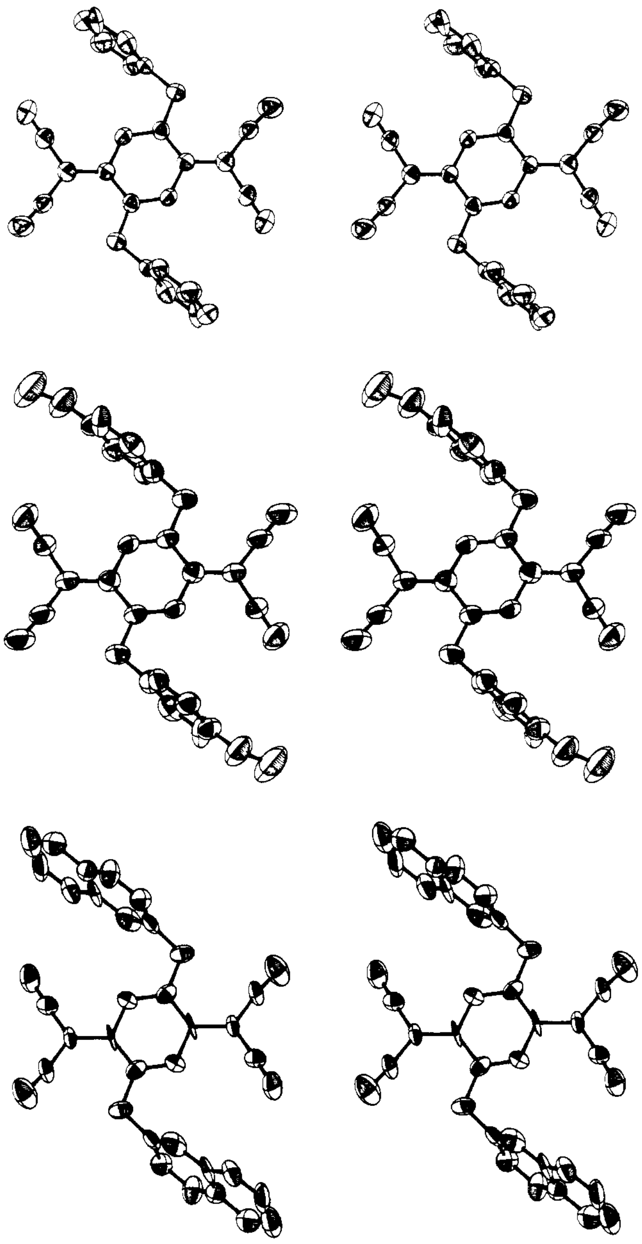

**Figure 2.** ORTEP stereo diagrams of the three molecules **2a**, **2b**, and **2c**. The molecule has been rotated out of plane 20° about the horizontal axis to facilitate viewing all the atoms.

---

[13] For a comprehensive review of segregated stack complexes, particularly $(TSeF)_x(TTF)_{1-x}$ TCNQ salts, see: *Highly Conducting One-Dimensional Solids*; Devreese, J. T., Ed.; Plenum: New York, 1978.

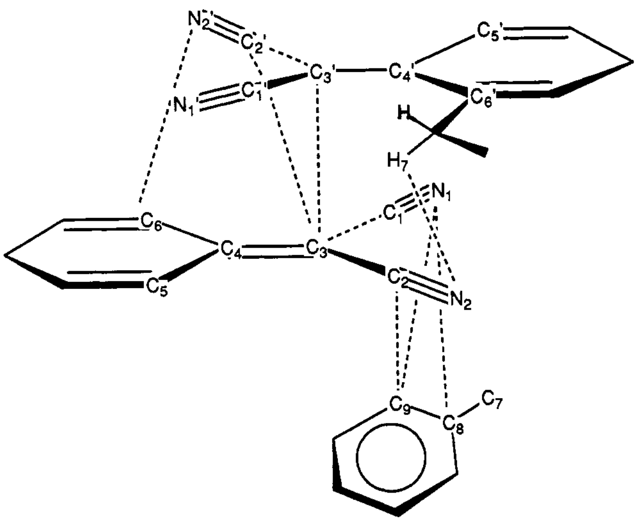

4

five N···C contacts less than 4.0 Å, the shortest being 3.68 (1) Å [3.584 (5) Å] between N2′ and C6 in **2c**. Similarly, there are 9, 5, and 7 C···C contacts less than 4.0 Å for **2a**, **2b**, and **2c**, respectively, within the same region, the shortest being 3.509 (5) Å between C3···C3′ in **2a**, with 3.524 (9) Å and 3.56 (1) Å [3.483 (5) Å] between C2···C3′ in **2b** and **2c**, respectively. In addition there are three N···H short contacts in all three compounds within a 3-Å distance, the shortest being 2.70 (1) Å [2.63 (3) Å] between N2···H7 in **2c** (see **4**). Irrespective of the nature of the donor moiety, this A···A stacking suggests that indeed the intramolecular connectivity of these molecules exerts sufficient driving force to push the TCNQ moieties toward this slipped segregated mode of stacking. Considering the D···A interactions in **4** within the 4-Å region in these three compounds, there are four N···C short contacts in each case between the acceptor nitrogens and donor carbons of the *c*-translated molecules. The shortest of these is 3.435 (6) and 3.64 (1) Å between N1···C9 in **2a** and **2b** and 3.50 (2) Å [3.432 (6) Å] between N1···C8 in **2c**.

We examine now the relationship between donors along this *c* stacking direction (Figure 3). For **2a** and **2b** there are no donor···donor distances less than 4.0 Å involving the phenyl rings. In **2b**, atoms on the methyl group are involved in several C···H and H···H interactions <4.0 Å, the shortest distances being 3.15 (8) Å {C13···H14B (*x*,*y*,1+*z*)} and 2.59 (9) Å {H13···H14B (*x*,*y*,1+*z*)}. In **2c**, however, the increased size of the donor allows for the possibility of increased overlap and the structure at least suggests the tendency for D···D stack formation with many distances less than 3.8 Å involving $\pi$-orbital interactions. Of the seven shortest C···H distances the most notable are 3.56 (2) Å [3.475 (7) Å] {C10···H14 (*x*,*y*,1+*z*)} and 3.31 (12) Å [3.26 (3) Å] between {C14···H10 (*x*,*y*,1+*z*)}, respectively. Thus **2c** is a step closer than **2a** and **2b** to a potentially perfect stacking situation schematized in **5**.

$$\begin{array}{ccccc} \cdot & & \cdot & & \cdot \\ \cdot & & \cdot & & \cdot \\ \text{D} & \text{-CH}_2\text{-} & \text{A} & \text{-CH}_2\text{-} & \text{D} \\ \cdot & & \cdot & & \cdot \\ \cdot & & \cdot & & \cdot \\ \cdot & & \cdot & & \cdot \\ \text{D} & \text{-CH}_2\text{-} & \text{A} & \text{-CH}_2\text{-} & \text{D} \\ \cdot & & \cdot & & \cdot \\ \cdot & & \cdot & & \cdot \end{array}$$

5

Now what about the charge-transfer interaction? The tendency for planar aromatic donors to form infinite mixed stacks with TCNQ clearly is not satified along the *c* axis. The D···A interactions are manifested through the formation of isolated D···A···D triplets in which the TCNQ unit of one molecule is flanked by two donor moieties of different neighboring molecules as shown in **3**. This may also be seen in stereo in Figure 3. In this view the upper dicyanomethylene group of the TCNQ at $^1/_2$,$^1/_2$,0 interacts with a donor group below it from the molecule at 1,1,0, while the lower dicyanomethylene group "sees" a donor from the molecule at the origin. Hence the interaction of these isolated D···A···D triplets is in the [110] direction. Since the molecule at $^1/_2$,$^1/_2$,0 is related to that at the origin by the screw axis, the same interaction must exist along the *c* axis, and this is shown for the "triplet" of molecules around the origin in Figure 3.

Why is there no infinite mixed stacking? Drawing **6** illustrates the structural constraints that prohibit such infinite D···A stacking. The stacking could have been established in a direction nearly perpendicular to the *c* direction where a triplet D···A···D already exists. Extension to an infinite stack is blocked by the TCNQ* moieties. Thus the unique D–CH$_2$–A–CH$_2$–D connectivity and the molecular conformation join together to replace the usual (D···A)$_\infty$ motif by D···A···D "triplets".

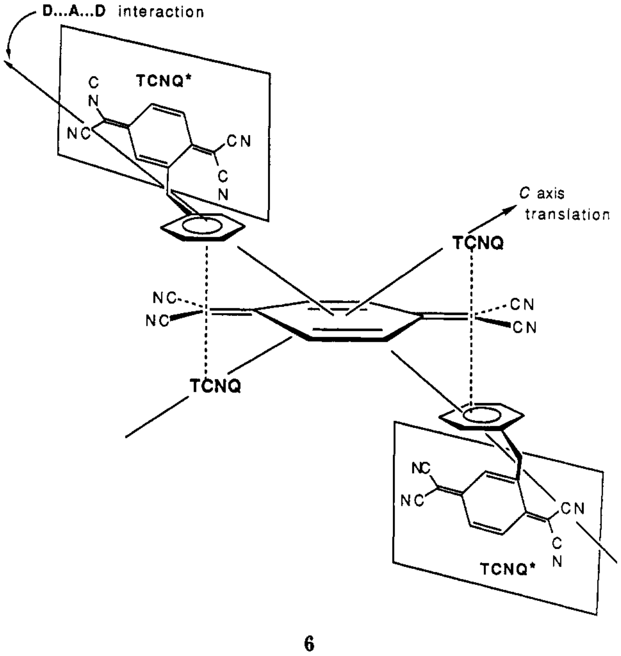

6

For both **2a** and **2c** the phenyl ring of a screw-related molecule very closely approaches a ring-over-bond type overlap with the double bond of the dicyanomethylene group. For **2c**, however, it is the "exterior" ring that participates in this overlap, leaving the "interior" ring to overlap with the C2–N2 bond. For **2b** the methoxy group plays the role of the "exterior" ring of **2c**. The hydrogens of the methoxy group inhibit good D···A···D $\pi$-overlap in this region. Consequently, the *p*-methoxy group bends outwards from its connected phenyl group, which results in the angle of 25° noted earlier between the plane of the phenyl ring and that of the methoxy group.

For **2b** this bending has some consequences for the intramolecular geometry, resulting in a considerably larger value for the angle between the methylene group and the quinone ring (Table V, planes 2 and 3) and a larger deviation from linearity for the N1–C1–C3 bond compared to **2a** and **2c**. Thus the energy involved in this strain in **2a** and **2c** can be compensated for by the greater overlap between the donor and acceptor moieties.

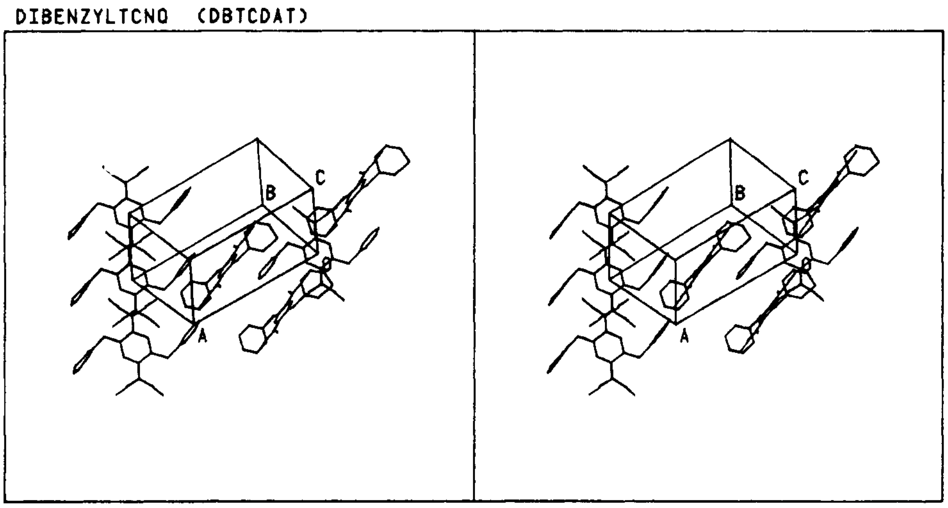

**Figure 3.** Packing diagram of **2a** showing the D···A···D interactions for the molecule at the origin and for the screw-related molecule in the middle of the *ab* face of the unit cell. This figure also shows the A···A overlap for the (1+$x$,1+$y$,$z$) translated molecule. Since the three structures are isomorphous, this packing diagram is a representative example of **2a**–**c**.

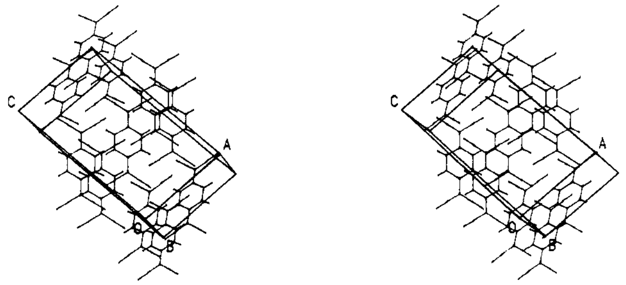

**Figure 4.** Packing diagram of TCNQ showing the molecular overlap in the *b* direction and neighboring screw-related molecules. The view is on the best plane of the molecule at the center of the cell.

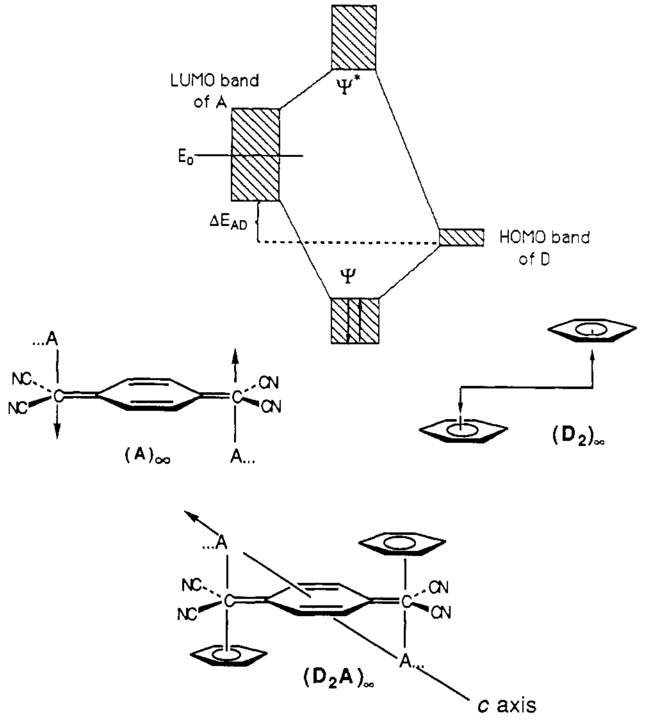

**Figure 5.** Simplified diagram for the interaction between the subbands of the LUMO of acceptor TCNQ and the HOMO of the aryl donor. On the left-hand side is shown the LUMO band of TCNQ. This subband is generated from the overlap of the LUMOs of the acceptor units in the *c* direction of the crystal. The band is relatively wide owing to the overlap between the LUMOs. Shown on the right-hand side is the subband of the HOMO of the aryl donor exemplified for the benzyl case. This subband is very narrow (except for the case of D = naphthyl) owing to the relatively poor overlap between units. The two bands interact owing to a nonzero overlap between the HOMO(D)-LUMO(A) and give rise to two bands with a mixed character, Ψ (filled) and Ψ* (empty), in the middle of the diagram. $E_0$ indicates the energy level of a free TCNQ. Thus the energy gap between the HOMO(D) and LUMO(A) subbands is smaller than the energy gap between the HOMO(D) and LUMO(A) of the free molecules.

The uniqueness of these structures is likely to find expression in the charge-transfer properties of the solids. Thus, the A···A interactions (LUMO(A)–LUMO(A), Figure 5) will join the D···A interactions (HOMO(D)–LUMO(A)) to enhance the mixing of charge-transfer configurations into the no-bond configuration and thereby increase the degree of charge transfer ($\rho$) more than in a weak mixed stack $(D\cdots A)_\infty$ complex made of free D and A moieties.[2] Indeed, the $\rho$ value of **2a** obtained from IR method of Chappel et al.[14] is $\approx$0.31, while either the bond lengths method of Kistenmacher et al.[15] or Coppens and Guru Row[16] or the method of Flaudrois and Classeau[17] yields a value of 0.26 (8) for **2a** and 0.2 (1) for **2b**. In the case of **2c**, the calculation yields an unreasonably large value of 0.7 (2), while the value obtained by all of these methods for the low-temperature data of **2c** are all much smaller. Except for the seemingly unreasonable discrepancy all indications are for $\rho$ = 0.2–0.3, which is approximately equal for **2a**–**c**. While these values should be viewed with a considerable degree of caution, there seems to be a correlation between packing pattern and some molecular geometric parameters. If they are meaningful, the $\rho$ values of **2a** and **2b** are higher than those of weak charge-transfer complexes and almost comparable to those of strong D···A pairs like TMTSF–TCNQ (red form).[18] An interesting comparison is between the $\rho$ values of $(D-CH_2)_2-A$ **2a**–**c** and those of their $(D\cdots A)_\infty$ analogues. Thus, for example, while $\rho$(**2c**) = 0.2–0.3, the same type of calculation yields

---

[14] Chappell, J. S.; Bloch, A. N.; Bryden, W. A.; Maxfield, M.; Poehler, T. O.; Cowan, D. O. *J. Am. Chem. Soc.* **1981**, *103*, 2442.

[15] Kistenmacher, T. J.; Emge, T. J.; Bloch, A. N.; Cowan, D. O. *Acta Crystallogr., Sect. B* **1982**, *38*, 1193.

[16] Coppens, P.; Guru Row, T. N. *Ann. N.Y. Acad Sci.* **1976**, *313*, 244.

[17] Flaudrois, F.; Classeau, K. *Acta Crystallogr., Sect. B* **1977**, *33*, 2744.

[18] Kistenmacher, T. J.; Phillips, T. E.; Cowan, D. O. *Acta Crystallogr., Sect. B* **1974**, *30*, 1193.

**Table II. Atomic Fractional Coordinates (×10$^4$ for Non-Hydrogen Atoms and ×10$^3$ for Hydrogen Atoms) in 2a, 2b, and 2c (at 93 K; ×10$^3$ for Non-Hydrogen Atoms and ×10$^2$ for Hydrogen Atoms in 2c) and Equivalent Thermal Parameters[a] (×10$^3$ for Non-Hydrogen Atoms and ×10$^2$ for Hydrogen Atoms) for Compounds 2a–c.**

| atom | $x$ | $y$ | $z$ | $U_{eq}$[a] | atom | $x$ | $y$ | $z$ | $U_{eq}$[a] |
|---|---|---|---|---|---|---|---|---|---|
| Compound **2a** | | | | | | | | | |
| N1 | −533 (3) | −2832 (4) | −5707 (5) | 75 (2) | C11 | 4061 (6) | 1558 (6) | −495 (10) | 87 (3) |
| N2 | 2001 (4) | −643 (4) | −4385 (6) | 75 (2) | C12 | 4036 (5) | 866 (5) | 1160 (9) | 76 (3) |
| C1 | −162 (3) | −2106 (4) | −4596 (5) | 52 (2) | C13 | 3222 (4) | 951 (4) | 1991 (7) | 56 (2) |
| C2 | −1312 (4) | −894 (4) | −3876 (5) | 49 (2) | H5 | 146 (3) | 34 (3) | −100 (5) | 4 (1) |
| C3 | 404 (3) | −1200 (3) | −3313 (5) | 45 (2) | H7A | 171 (3) | 150 (4) | 350 (6) | 6 (1) |
| C4 | 153 (3) | −641 (3) | −1689 (5) | 40 (2) | H7B | 130 (3) | 263 (4) | 201 (6) | 6 (1) |
| C5 | 851 (3) | 228 (4) | −608 (5) | 43 (2) | H9 | 200 (3) | 306 (4) | −91 (6) | 6 (1) |
| C6 | 746 (3) | 860 (3) | 1012 (5) | 42 (2) | H10 | 332 (3) | 292 (4) | −242 (7) | 8 (2) |
| C7 | 1541 (3) | 1751 (4) | 2041 (6) | 51 (2) | H11 | 466 (4) | 152 (5) | −98 (8) | 12 (3) |
| C8 | 2443 (3) | 1722 (3) | 1204 (5) | 44 (2) | H12 | 464 (4) | 28 (4) | 196 (8) | 13 (2) |
| C9 | 2499 (4) | 2441 (4) | −428 (6) | 58 (2) | H13 | 320 (3) | 40 (4) | 310 (6) | 7 (1) |
| C10 | 3307 (5) | 2342 (5) | −1280 (7) | 75 (3) | | | | | |
| Compound **2b** | | | | | | | | | |
| O1 | 4222 (3) | 1218 (6) | −102 (7) | 103 (3) | C11 | 3486 (4) | 1464 (8) | 325 (11) | 67 (4) |
| N1 | −533 (4) | −3181 (8) | −5345 (10) | 105 (5) | C12 | 3425 (5) | 833 (8) | 1961 (12) | 69 (5) |
| N2 | 1536 (4) | −695 (7) | −4264 (1) | 96 (4) | C13 | 2722 (4) | 1009 (8) | 2490 (12) | 60 (4) |
| C1 | −193 (4) | −2364 (8) | −4351 (1) | 70 (4) | C14 | 4231 (11) | 1357 (25) | −1985 (23) | 150 (13) |
| C2 | 993 (4) | −982 (7) | −3706 (9) | 62 (4) | H5 | 116 (3) | 42 (5) | −73 (7) | 5 (2) |
| C3 | 285 (4) | −1339 (9) | −3146 (9) | 54 (4) | H7A | 150 (4) | 182 (7) | 368 (9) | 10 (2) |
| C4 | 109 (3) | −719 (6) | −1609 (9) | 52 (3) | H9 | 174 (3) | 293 (6) | −77 (8) | 5 (2) |
| C5 | 699 (3) | 229 (6) | −526 (9) | 55 (3) | H10 | 292 (1) | 278 (1) | −206 (1) | 4 (1) |
| C6 | 629 (3) | 934 (6) | 987 (9) | 52 (3) | H12 | 394 (3) | 32 (5) | 291 (8) | 6 (2) |
| C7 | 1301 (4) | 1909 (7) | 2074 (10) | 67 (4) | H13 | 271 (4) | 55 (6) | 355 (9) | 7 (2) |
| C8 | 2083 (4) | 1800 (7) | 1451 (10) | 56 (4) | H14A | 475 (4) | 121 (6) | −198 (9) | 7 (2) |
| C9 | 2173 (5) | 2440 (8) | −129 (13) | 69 (5) | H14B | 372 (6) | 107 (9) | −301 (1) | 14 (4) |
| C10 | 2868 (5) | 2288 (8) | −764 (11) | 79 (5) | H14C | 407 (7) | 205 (9) | −191 (2) | 6 (5) |
| Compound **2c** | | | | | | | | | |
| N1 | 54 (1) | −263 (1) | 580 (2) | 87 (7) | C14 | −369 (2) | 244 (2) | 209 (3) | 97 (13) |
| N2 | −169 (1) | −53 (1) | 362 (1) | 74 (6) | C15 | −301 (1) | 264 (1) | 162 (2) | 65 (8) |
| C1 | 20 (1) | −199 (1) | 459 (1) | 48 (6) | C16 | −295 (1) | 203 (1) | −5 (2) | 50 (7) |
| C2 | −107 (1) | −81 (1) | 341 (2) | 43 (7) | C17 | −361 (1) | 126 (1) | −118 (2) | 54 (8) |
| C3 | −31 (1) | −112 (1) | 313 (1) | 40 (6) | H5 | −16 (1) | 2 (1) | −3 (1) | 9 (4) |
| C4 | −10 (1) | −58 (1) | 160 (1) | 43 (6) | H7A | −12 (1) | 26 (1) | −23 (1) | 9 (4) |
| C5 | −75 (1) | 21 (1) | 29 (1) | 43 (5) | H7B | −15 (1) | 13 (1) | −40 (2) | 14 (5) |
| C6 | −67 (7) | 82 (1) | −127 (1) | 46 (6) | H8 | −18 (1) | 26 (1) | 3 (1) | 1 (2) |
| C7 | −139 (1) | 162 (1) | −264 (2) | 51 (6) | H10 | −27 (1) | 4 (1) | −46 (2) | 12 (5) |
| C8 | −224 (1) | 218 (1) | −65 (2) | 62 (9) | H11 | −39 (1) | 0 (1) | −34 (2) | 6 (4) |
| C9 | −217 (1) | 154 (1) | −222 (2) | 45 (6) | H12 | −50 (1) | 7 (1) | −18 (1) | 1 (2) |
| C10 | −287 (1) | 77 (1) | −331 (2) | 57 (8) | H13 | −49 (1) | 16 (1) | 14 (1) | 24 (10) |
| C11 | −357 (1) | 64 (1) | −281 (2) | 72 (9) | H14 | −39 (1) | 29 (1) | 28 (2) | 11 (6) |
| C12 | −435 (1) | 112 (1) | −65 (2) | 78 (9) | H15 | −24 (1) | 30 (1) | 24 (1) | 4 (3) |
| C13 | −438 (1) | 170 (1) | 100 (3) | 96 (11) | | | | | |
| Compound **2c** (at 93 K) | | | | | | | | | |
| N1 | −547 (2) | −2660 (2) | 4788 (5) | 31 (2) | C14 | 3699 (3) | 2484 (3) | 9537 (7) | 38 (2) |
| N2 | 1698 (2) | −508 (2) | 7044 (5) | 31 (2) | C15 | 3008 (2) | 2665 (3) | 7622 (6) | 34 (2) |
| C1 | −195 (2) | −1972 (3) | 4246 (5) | 23 (2) | C16 | 3641 (2) | 1267 (3) | 6049 (6) | 26 (2) |
| C2 | 1097 (2) | −785 (3) | 5579 (6) | 28 (2) | C17 | 2971 (2) | 2052 (3) | 5856 (6) | 28 (2) |
| C3 | 310 (2) | −1113 (2) | 3744 (6) | 22 (2) | H5 | 130 (2) | 33 (3) | 299 (5) | 3 (1) |
| C4 | 120 (2) | −595 (2) | 1864 (5) | 20 (2) | H7A | 118 (2) | 240 (3) | −12 (5) | 2 (1) |
| C5 | 52 (2) | 224 (2) | 1756 (6) | 22 (2) | H7B | 160 (3) | 137 (4) | −91 (7) | 6 (2) |
| C6 | 678 (2) | 812 (2) | 45 (5) | 22 (2) | H8 | 179 (2) | 277 (2) | 380 (4) | 1 (1) |
| C7 | 1395 (2) | 1633 (3) | 104 (7) | 27 (2) | H10 | 283 (2) | 33 (3) | 103 (7) | 5 (1) |
| C8 | 2250 (2) | 2213 (3) | 3840 (6) | 29 (2) | H11 | 413 (2) | 6 (3) | 459 (5) | 3 (1) |
| C9 | 2205 (2) | 1581 (3) | 2177 (6) | 25 (2) | H12 | 486 (2) | 64 (2) | 822 (5) | 1 (1) |
| C10 | 2887 (2) | 791 (3) | 2396 (6) | 28 (2) | H13 | 492 (3) | 164 (4) | 1102 (8) | 8 (2) |
| C11 | 3595 (2) | 644 (3) | 4295 (6) | 29 (2) | H14 | 378 (3) | 296 (4) | 1078 (7) | 6 (1) |
| C12 | 4364 (2) | 1113 (3) | 8076 (7) | 34 (2) | H15 | 251 (2) | 316 (3) | 728 (5) | 2 (1) |
| C13 | 4386 (2) | 1714 (3) | 9741 (6) | 30 (3) | | | | | |

[a] $U_{eq} = (U_{11}U_{22}U_{33})^{1/3}$. $\sigma(U_{eq}) = [\sigma^2 U_{11}(U_{22}U_{33})^{1/3}(^1/_3 U_{11}{}^{-2/3}) + \sigma^2 U_{22}(U_{11}U_{33})^{1/3}(^1/_3 U_{22}{}^{-2/3}) + \sigma^2 U_{33}(U_{22}U_{11})^{1/3}(^1/_3 U_{33}{}^{-2/3})]^{1/2}$. [b] Estimated standard deviations for the last significant figure are given in parentheses.

a $\rho$ value of 0.15 (8) for the naphthalene–TCNQ 1:1 mixed stack complex.[19] The enhanced degree of charge transfer in **2c** could be the result of the stacking of the TCNQ moieties which in turn enhances the interaction of the $\pi^*$ levels with the weak donorlike naphthalene relative to its interactions with the $\pi^*$ level of isolated TCNQ in the naphthalene–TCNQ complex. In the mixed stack (naphthalene:TCNQ)$_\infty$ complex there is no TCNQ–TCNQ overlap as observed in **2c**. Thus the energy gap between $\pi^*$ (LUMO) of separate TCNQ and the $\pi$ (HOMO) of naphthalene is sufficiently large to cause only a small transfer of charge. On the other hand, in **2c** the formation of a band due to overlapping TCNQs provides a set of lower energy LUMO levels accessible for transfer of charge. Thus, the D–CH$_2$–A–CH$_2$–D structure is seen to offer a

---

(19) Tickle, I. J.; Prout, C. K. *J. Chem. Soc., Perkin Trans 2* **1973**, 720. Hanson, A. W. *Acta Crystallogr., Sect. B* **1978**, *34*, 2339.

**Table III. Geometric Parameters for the TCNQ Unit in Compounds 2a–c and Neat TCNQ**

| | **2a** | **2b** | **2c** | **2c** (at 93 K) | TCNQ[10] |
|---|---|---|---|---|---|
| | | Bond Lengths, Å | | | |
| N1–C1 | 1.143 (6) | 1.134 (9) | 1.11 (2) | 1.145 (4) | 1.141 (3) |
| N2–C2 | 1.130 (7) | 1.145 (9) | 1.17 (5) | 1.143 (5) | 1.139 (3) |
| C1–C3 | 1.438 (5) | 1.439 (9) | 1.45 (2) | 1.428 (4) | 1.441 (4) |
| C2–C3 | 1.450 (7) | 1.420 (9) | 1.42 (2) | 1.444 (5) | 1.440 (4) |
| C3–C4 | 1.391 (5) | 1.381 (9) | 1.42 (1) | 1.384 (5) | 1.374 (3) |
| C4–C5 | 1.441 (5) | 1.436 (8) | 1.45 (2) | 1.443 (4) | 1.446 (4) |
| C5–C6 | 1.353 (5) | 1.338 (9) | 1.37 (1) | 1.345 (5) | 1.346 (3) |
| C4–C6[a] | 1.456 (6) | 1.462 (7) | 1.45 (2) | 1.465 (4) | 1.450 (4) |
| C6–C7 | 1.525 (6) | 1.533 (9) | 1.52 (2) | 1.515 (4) | |
| | | Bond Angles, deg | | | |
| N1–C1–C3 | 173.1 (4) | 176.0 (7) | 173.1 (13) | 174.4 (4) | 179.4 (2) |
| N2–C2–C3 | 177.3 (4) | 176.2 (7) | 178.3 (12) | 177.2 (4) | 179.6 (2) |
| C1–C3–C2 | 112.5 (3) | 112.5 (6) | 112.8 (9) | 112.5 (3) | 116.1 (2) |
| C1–C3–C4 | 126.8 (4) | 126.6 (6) | 125.8 (10) | 127.6 (3) | 112.0 (2) |
| C2–C3–C4 | 120.8 (3) | 120.8 (6) | 121.4 (9) | 119.8 (3) | 121.8 (2) |
| C3–C4–C5 | 116.4 (4) | 117.3 (5) | 114.1 (10) | 117.5 (3) | 121.0 (2) |
| C3–C4–C6′[a] | 125.5 (3) | 125.8 (5) | 124.7 (9) | 124.7 (3) | 120.7 (2) |
| C5–C4–C6′[a] | 118.1 (3) | 116.8 (5) | 121.2 (9) | 117.8 (3) | 118.3 (2) |
| C4–C5–C6 | 125.3 (4) | 125.8 (5) | 123.4 (10) | 125.8 (3) | 121.0 (2) |
| C5–C6–C4′[a] | 116.5 (3) | 117.4 (5) | 115.4 (9) | 116.4 (3) | 120.7 (2) |
| C5–C6–C7 | 120.5 (4) | 121.9 (5) | 121.1 (10) | 121.2 (3) | |
| C4A–C6–C7 | 112.9 (3) | 120.6 (5) | 123.3 (9) | 122.4 (3) | |

[a] C6′ is centrosymmetrically related to C6 and similarly C4′.

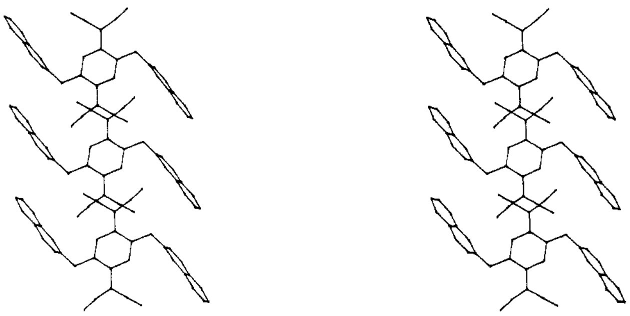

Figure 6. Stacking diagram of the molecule **2c** showing the overlap of acceptor moieties within a stack. The small but significant overlap between the donor naphthyl units can also be seen.

unique opportunity for segregating stacking on the one hand and for D···A interactions, on the other hand. Moreover, both interaction types seem to intensify each other. This culminated in **2c** with the D = naphthyl case which exhibits $(D)_\infty$, $(A)_\infty$ stacking, **5**, along with D···A···D interaction.

**Lattice Energy Minimization Calculations for 2a–c.** Lattice energy calculations have been employed increasingly over the past few years in attempts to understand in greater detail the nature of crystal packing regularities (and irregularities).[20] This case of three molecules with different steric properties at the extremities but that nevertheless crystallize isostructurally appeared to be an excellent candidate for investigation by this technique.

The results of the lattice energy minimization calculations carried out for the three compounds **2a–c** and TCNQ are tabulated in Table VI. Before discussing the trends in the calculations, one comment about their reliability is

**Table IV. Bond Lengths and Angles in the Donor Units of 2a–c**[a]

| | | | | | | | |
|---|---|---|---|---|---|---|---|
| | | | Bond Lengths and Angles in **2a** | | | | |
| C7–C8 | 1.502 (6) | C8–C9 | 1.392 (5) | C8–C13 | 1.385 (6) | C9–C10 | 1.391 (8) |
| C10–C11 | 1.37 (1) | C11–C12 | 1.380 (9) | C12–C13 | 1.389 (9) | | |
| C6–C7–C8 | 113.2 (3) | C7–C8–C9 | 120.5 (4) | C7–C8–C13 | 121.0 (4) | | |
| C9–C8–C13 | 118.5 (4) | C8–C9–C10 | 120.1 (4) | C9–C10–C11 | 120.3 (5) | | |
| C10–C11–C12 | 120.6 (7) | C11–C12–C13 | 119.0 (6) | | | | |
| | | | Bond Lengths and Angles in **2b** | | | | |
| C7–C8 | 1.521 (9) | C8–C9 | 1.36 (1) | C8–C13 | 1.37 (1) | C9–C10 | 1.39 (1) |
| C10–C11 | 1.38 (1) | C11–C12 | 1.37 (1) | C12–C13 | 1.36 (1) | C11–O1 | 1.390 (8) |
| O1–C14 | 1.36 (2) | | | | | | |
| C6–C7–C8 | 112.1 (5) | C7–C8–C9 | 122.6 (6) | C7–C8–C13 | 119.5 (6) | | |
| C9–C8–C13 | 117.9 (7) | C8–C9–C10 | 122.7 (7) | C9–C10–C11 | 116.7 (7) | | |
| C10–C11–C12 | 122.0 (7) | C11–C12–C13 | 118.4 (7) | C10–C11–O1 | 123.8 (7) | | |
| C12–C11–O1 | 114.2 (7) | C11–O1–C14 | 118.7 (9) | | | | |
| | | | Bond Lengths and Angles in **2c** | | | | |
| C7–C9 | 1.48 (2) | C8–C9 | 1.38 (2) | C8–C16 | 1.45 (2) | C9–C10 | 1.42 (2) |
| C10–C11 | 1.39 (2) | C11–C17 | 1.39 (2) | C12–C13 | 1.37 (2) | C12–C17 | 1.46 (2) |
| C13–C14 | 1.40 (3) | C14–C15 | 1.35 (3) | C15–C16 | 1.42 (2) | C16–C17 | 1.40 (2) |
| C6–C7–C9 | 112 (1) | C7–C9–C8 | 120 (1) | C7–C9–C10 | 123 (1) | | |
| C9–C8–C16 | 122 (1) | C8–C9–C10 | 117 (1) | C9–C10–C11 | 123 (1) | | |
| C10–C11–C17 | 120 (1) | C11–C17–C16 | 121 (1) | C17–C16–C8 | 118 (1) | | |
| C8–C16–C15 | 122 (1) | C17–C16–C15 | 119 (1) | C11–C17–C12 | 120 (1) | | |
| C16–C17–C12 | 120 (1) | C16–C15–C14 | 119 (2) | C17–C12–C13 | 120 (2) | | |
| C12–C13–C14 | 118 (2) | C13–C14–C15 | 125 (2) | | | | |
| | | | Bond Lengths and Angles in **2c** (at 93 K) | | | | |
| C7–C9 | 1.521 (5) | C8–C9 | 1.357 (5) | C–C16 | 1.438 (5) | C9–C10 | 1.416 (5) |
| C10–C11 | 1.375 (5) | C11–C17 | 1.406 (5) | C12–C13 | 1.352 (6) | C12–C17 | 1.444 (5) |
| C13–C14 | 1.410 (5) | C14–C15 | 1.375 (6) | C15–C16 | 1.412 (5) | C16–C17 | 1.401 (5) |
| C6–C7–C9 | 112.2 (3) | C7–C9–C8 | 120.9 (3) | C7–C9–C10 | 118.8 (3) | | |
| C9–C8–C16 | 120.4 (3) | C8–C9–C10 | 120.1 (3) | C9–C10–C11 | 120.6 (3) | | |
| C10–C11–C17 | 120.1 (3) | C11–C17–C16 | 120.0 (3) | C17–C16–C8 | 118.8 (3) | | |
| C8–C16–C15 | 121.1 (3) | C17–C16–C15 | 120.1 (3) | C11–C17C12 | 121.6 (3) | | |
| C16–C17–C12 | 118.5 (3) | C16–C15–C14 | 120.0 (3) | C17–C12–C13 | 120.3 (3) | | |
| C12–C13–C14 | 120.7 (4) | C13–C14–C15 | 120.4 (4) | | | | |

[a] Estimated standard deviations for the last significant figures are given in parentheses.

Table V. Plane Definitions and Angles between Normals to the Planes

| | |
|---|---|
| plane 1: | N1 N2 C1 C2 C3, **2a–c** |
| plane 2: | C4 C5 C6 C4′ C5′ C6′, **2a–c** |
| plane 3: | C6 C7 C8, **2a–b**<br>C6 C7 C9, **2c** |
| plane 4: | C8 C9 C10 C11 C12 C13 **2a–b**<br>C8 C9 C10 C11 C12 C13 C14 C15 C16 C17 **2c** |

| compd | plane 1-plane 2 | plane 2-plane 3 | plane 2-plane 4 | plane 3-plane 4 |
|---|---|---|---|---|
| **2a** | 178.2 | 173.9 | 96.1 | 85.8 |
| **2b** | 174.9 | 161.8 | 96.2 | 77.4 |
| **2c** | 177.0 | 171.6 | 94.6 | 85.6 |
| **2c** (at 93 K) | 176.2 | 172.8 | 95.9 | 85.0 |

in order. As one would expect, the cell parameters for the minimized structure of **2c** are consistently shifted in the direction of the low-temperature structure of **2c**, which contributes considerably to our confidence in the calculations.

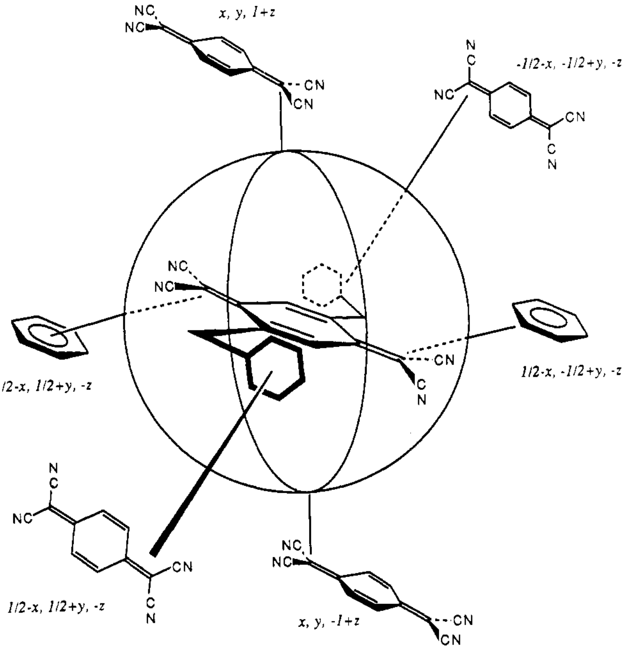

**7**

Since the energetics are determined by nearest neighbors, it is useful to dwell briefly on some additional details of the "coordination sphere" of a single (reference) molecule **7**; this will also aid in the analysis of the lattice energy calculations. Each of the molecules of **2a–c** is surrounded by six neighbors. Within an acceptor stack there is one acceptor unit below the reference molecule and one above it at the positions $\{x,y,1+z;\ x,y,-1+z\}$. The reference molecule overlaps in a similar fashion with donor units of molecules $\{0.5-x,-0.5+y,-z;\ -0.5-x,0.5+y,-z\}$. The donor units of the reference molecule also make a similar overlap with the two acceptor units of two other different molecules $\{0.5-x,0.5+y,-z;\ -0.5-x,-0.5+y,z\}$. Hence these six molecules constitute the first coordination sphere. In contrast, in TCNQ solid there are 10 molecules in the coordination sphere (Figure 4), and in the absence of stacking, it appears that the dominant interaction is dipole–dipole.

Through the "series" of structures **2a–c**, even though the A···A overlap is nearly constant, the D···A overlap is slightly different as discussed earlier. In **2b** the D···A interactions mimic the overlap of that of **2c**. This is indicated by the lattice energy which is more similar for these two compounds than to that of **2a**. In fact the values are considerably closer when considering only the van der Waals energy, and the excess energy for **2b** compared to **2c** is primarily from the electrostatic contribution of the oxygen atom.

The total energy can also be partitioned to obtain energy contributions due to the interaction of various molecules with the reference molecule, represented schematically in **7**. In going from **2a** to **2c** there is a continuous increase in the energy contribution from the two nearest-neighbor molecules in the stacking direction (Table VI). The reason for this increase is that even though the A···A overlap is similar in all three, as the size of the donor group increases from **2a** to **2c**, there is an increasing number of D···D interactions in the form of C···H and C···C interactions as noted earlier. This partitioning provides quantitative support for the qualitative structural arguments presented above.

When one considers the contributions of screw-related molecules that optimize D···A interactions, their contributions in **2b** are greater than in **2c**, which in turn are slightly greater than in **2a**. However, the electrostatic contribution to these values is greater in **2b** and is nearly the same for **2a** and **2c**. The contribution by the four screw-related molecules in **2c** is slightly more than the value in **2a** because the former contains a larger number of carbon atoms in its donor unit, which results in a larger number of D···A interactions. The van der Waals contributions of screw-related molecules in **2b** and **2c** are very similar (−5.12 and −5.15 kcal $\mathrm{mol^{-1}}$, respectively), which is again consistent with the notion of the *p*-methoxy group mimicking the behavior of naphthalene. Again, owing to the presence of an oxygen atom in the donor unit, the electrostatic contribution is larger in **2b** and hence the net contribution by the screw-related molecules in **2b** is more than that in **2c**. Although there are some subtle yet apparent differences in the packing arrangements of these three compounds, the total contributions by the six molecules (two forming A···A and four forming D···A interactions comprising the first coordination sphere) to their respective total lattice energies are very similar, which is the energetic manifestation of the isostructurality of these three compounds. Yet the absolute magnitude of this contribution increases in going from **2a** to **2c**, thus indicating the interplay of A···A and D···A interactions probably due to the orbital interactions discussed above.

The contributions of various individual atoms to the total energies are also given in Table VI. To aid in the analyses, only those atoms that are common in all the three compounds are listed save the oxygen of **2b**. The contribution of the oxygen atom to the total energy in **2b** is −16.23 kcal $\mathrm{mol^{-1}}$, which is greater than any other single atomic contribution. This high value is clearly due to its significant electrostatic contribution.

The relative contributions of common atoms in these three structures are nearly the same except for two atoms N2 and the methylene hydrogen H7B in **2b**. This is consistent with our observation that the D···A overlap in **2b** is slightly different from that in the other compounds (Figure 6) where the donor phenyl group is directly

---

(20) Williams, D. E. *Top. Appl. Phys.* **1981**, *26*, 3. Kitaigorodskii, A. I. *Molecular Crystals and Molecules*; Academic Press: New York, 1983. Bernstein, J. In *Organic Solid State Chemistry*; Desiraju, G. R., Ed.; Elsevier: New York, 1987.

(21) Williams, D. E.; Cox, S. R. *Acta Crystallogr., Sect. B.* **1984**, *40*, 404. Cox, S. R.; Hsu, L. Y.; Williams, D. E. *Acta Crystallogr., Sect. A* **1981**, *37*, 293.

(22) Ermer, O. *Struct. Bonding* **1976**, *27* 163.

(23) Mirsky, K. *Acta Crystallogr., Sect. A* **1976**, *32*, 199.

(24) Allinger, N. L. *Adv. Phys. Org. Chem.* **1976**, *12*, 2.

**Table VI. Lattice Energy Minimization Calculations on 2a–c and Neat TCNQ[a]**

| | 2a | 2b | 2c | TCNQ |
|---|---|---|---|---|
| initial energy, kcal/mol | −48.5 (−3.18) | −66.0 (−9.42) | −60.2 (−4.98) | −22.8 (−1.55) |
| final energy | −48.9 (−3.59) | −69.5 (−12.5) | −60.7 (−5.32) | −23.4 (−1.27) |
| cell parameters[b] | | | | |
| *a*, Å | 14.23 (0.24) | 16.47 (−0.41) | 16.79 (−0.15) | 8.72 (−0.19) |
| *b*, Å | 10.92 (0.15) | 9.68 (−0.56) | 11.64 (−0.04) | 6.77 (−0.29) |
| *c*, Å | 6.77 (−0.20) | 7.60 (0.43) | 7.07 (−0.02) | 17.54 (1.14) |
| $\beta$, deg | 103.9 (1.4) | 111.1 (3.3) | 115.1 (0.8) | 100.9 (2.4) |
| $V$, Å$^3$ | 999.5 (−25.5) | 1054.0 (−125.6) | 1133.7 (−144.0) | 999.7 (−10.5) |
| Contributions from Neighboring Molecules, kcal/mol | | | | |
| all stacking molecules[c] | −9.05 (−4.14)[a] | −10.80 (−5.28) | −12.86 (−6.09) | −7.26 |
| A···A interactions | −8.70 (−4.04) | −8.25 (−3.83) | −9.01 (−4.42) | |
| D···D interactions | −0.35 (−0.10) | −2.55 (−1.45) | −3.85 (−1.67) | |
| screw-related molecules[d] (D···A) interaction | −4.62 (−0.24) | −7.76 (−2.64) | −5.50 (−0.32) | −5.36 |
| net % contribution from first coord sphere[e] (see 7) | 75.4 | 75.7 | 78.6 | 69.3 |
| Partitioned Atomic Contributions, kcal/mol | | | | |
| N1 | −9.56 | −8.28 | −7.75 | −3.33 |
| N2 | −10.86 | −13.38 | −9.08 | −5.10 |
| C1 | 3.60 | 1.90 | 2.28 | −1.86 |
| C2 | 4.46 | 4.47 | 3.17 | −1.59 |
| C3 | 1.33 | 0.54 | 0.44 | −2.25 |
| C4 | 0.69 | 0.61 | 0.15 | −2.17 |
| C5 | −1.35 | −1.21 | −1.21 | −2.40 |
| C6 | 0.64 | 0.92 | 0.88 | −2.30 |
| C7 | −1.28 | −1.18 | −1.17 | |
| H5 | 0.17 | 0.17 | 0.05 | −0.02 |
| H7A | 0.10 | 0.05 | 0.11 | |
| H7B | 0.01 | 0.34 | 0.05 | |
| O1 | | −16.23 | | |

[a] Electrostatic contributions to the total energy on the previous lines are given in parentheses. [b] Deviations from experimental values in parentheses. [c] Contribution from one of the acceptor molecules at either $x,y,-1+z$ or $x,y,1+z$. [d] Contribution from one of the molecules at positions $0.5-x$, $-0.5+y,-z$, $-0.5-x$, $0.5+y$, $-z$; $0.5-x$, $0.5+y$, $-z$, or $-0.5-x$, $-0.5+y$, $-z$, which give rise to D···A interactions. [e] Sum of the six molecules in c and d (see 7) as a percentage of the total lattice energy.

overlapping with the N2–C2 nitrile bond and hence the N2 is in a more favorable energetic environment. In a similar fashion, the methylene bridge which connects the donor moiety to the quinonoid ring makes an angle of 18° with the latter, and its hydrogens, relieved from the steric strain, are stabilized by a greater extent compared to the other two molecules.

An alternative way of viewing compounds **2a–c** is simply as substituted TCNQs. As we have shown above, the geometric features of the packing (Figure 3 vs Figure 4) clearly provide strong structural evidence against such a view. These lattice energy calculations also argue against this interpretation. The partitioned energy for the atoms of unsubstituted TCNQ (Table VI) have characteristics significantly different from those of **2a–c**, indicating also that a very different set of interactions is operating here. For instance, for TCNQ, the lattice energy may be thought of as arising from a cooperative effect of virtually all the atoms. Clearly in **2a–c** the nitrile nitrogens play an important role in the stabilization of the crystal. Increasing that role, reducing the destabilizing role of the carbon atoms, and, for example, finding polar substituents such as the methoxy oxygen are routes to be considered for obtaining this type of packing.

## Conclusions

We have presented here the crystal and molecular structures of three isostructural molecules that form the basis for a family of π-charge-transfer compounds wherein donor and acceptor moieties are chemically linked. The linkage in this case is through electronically insulating methylene groups connecting two aromatic hydrocarbons to a TCNQ acceptor in a mode which leads to $C_i$ point symmetry for the molecule. In the crystal these materials adopt a packing motif that differs considerably from that of TCNQ with incipient *segregated stacking* of the acceptor moieties. These materials thus satisfy one of the architectural requirements for electrical conductivity in π EDA complexes.[1] The charge transfer is satisfied by the formation of isolated D···A···D sandwich "triads" rather than infinite mixed stacks, which also comprises a new packing motif. The compounds studied here are not conductors due to the low degree of the transfer of charge. Lattice energy calculations, including partitioning into individual atomic contributions, provide insight into some of the dominant intermolecular interactions in these structures and serve as an aid in the continuing design of potentially electrically conducting materials based on molecules composed of chemically linked donor and acceptor moieties. Increasing the degree of charge transfer by suitable chemical modification of both donor and acceptor moieties within this promising molecular motif is currently under way.

**Acknowledgment.** We thank Dr. Felix Frolow of the Weizmann Institute of Science for providing us with the low-temperature data set. Financial support from the Germany–Israel Cooperative Research Program administered by the Israel National Council for Research and Development and from the United States Army European Office of Research are greatly appreciated. Finally we thank Michael Dorfman and Yaron Danon for their very able technical assistance.

**Registry No.** **2a**, 85421-78-9; **2b**, 113475-14-2; **2c**, 113475-16-4.

**Supplementary Material Available:** Listings of torsion angles and atomic charges (14 pages) and structure factors (23 pages) for compounds **2a–c**. Ordering information is given on any current masthead page.